THE JOURNAL OF BIOLOGICAL CHEMISTRY VOL. 283, NO. 43, pp. 29086–29098, October 24, 2008

N-Glycan-mediated Quality Control in the Endoplasmic Reticulum Is Required for the Expression of Correctly Folded δ-Opioid Receptors at the Cell Surface*[S]

Received for publication, March 7, 2008, and in revised form, July 16, 2008 Published, JBC Papers in Press, August 14, 2008, DOI 10.1074/jbc.M801880200

Piia M. H. Markkanen and Ulla E. Petäjä-Repo[1]

From the Department of Anatomy and Cell Biology, Institute of Biomedicine, University of Oulu, FI-90014, Oulu, Finland

A great majority of G protein-coupled receptors are modified by *N*-glycosylation, but the functional significance of this modification for receptor folding and intracellular transport has remained elusive. Here we studied these phenomena by mutating the two N-terminal *N*-glycosylation sites (Asn^{18} and Asn^{33}) of the human δ-opioid receptor, and expressing the mutants from the same chromosomal integration site in stably transfected inducible HEK293 cells. Both *N*-glycosylation sites were used, and their abolishment decreased the steady-state level of receptors at the cell surface. However, pulse-chase labeling, cell surface biotinylation, and immunofluorescence microscopy revealed that this was not because of intracellular accumulation. Instead, the non-*N*-glycosylated receptors were exported from the endoplasmic reticulum with enhanced kinetics. The results also revealed differences in the significance of the individual *N*-glycans, as the one attached to Asn^{33} was found to be more important for endoplasmic reticulum retention of the receptor. The non-*N*-glycosylated receptors did not show gross functional impairment, but flow cytometry revealed that a fraction of them was incapable of ligand binding at the cell surface. In addition, the receptors that were devoid of *N*-glycans showed accelerated turnover and internalization and were targeted for lysosomal degradation. The results accentuate the importance of protein conformation-based screening before export from the endoplasmic reticulum, and demonstrate how the system is compromised when *N*-glycosylation is disrupted. We conclude that *N*-glycosylation of the δ-opioid receptor is needed to maintain the expression of fully functional and stable receptor molecules at the cell surface.

Secreted and membrane-bound proteins are co-translationally inserted into the endoplasmic reticulum (ER),[2] where they are immediately subjected to scrutiny by the ER quality control machinery. It ensures that only proteins with native conformation are transported to their final destinations. This is achieved by aiding the folding of nascent protein molecules and retaining and targeting aberrant folding products for degradation (1). The glycoprotein quality control is an essential part of general ER quality control. It relies on *N*-linked glycosylation, which occurs on asparagine residues at the Asn-*X*-(Ser/Thr) consensus sequence (where *X* is any amino acid except proline) of a folding substrate, as it emerges into the ER (2, 3). Removal of two glucose residues from the core *N*-glycans allows the nascent glycoprotein to interact with ER-localized molecular chaperones calnexin and calreticulin, and subsequent release and rebinding to these chaperones is regulated by two enzymes, glucosidase II and UDP-glucose:glycoprotein glycosyltransferase, that remove and add glucose to the core glycan, respectively (3, 4). The latter enzyme recognizes folding intermediates but disregards native proteins and substrates that are targeted for ER-associated degradation because of terminal misfolding. This so-called calnexin cycle retains incompletely folded proteins in the ER and with the help of interacting foldases, like protein-disulfide isomerase family member ERp57, assists in folding.

G protein-coupled receptors (GPCRs) are membrane proteins that, apart from a few exceptions, contain several consensus sites for *N*-glycosylation in their extracellular domains (5). They are therefore obvious targets for ER glycoprotein quality control. Nevertheless, the functional significance of their *N*-glycans in folding and intracellular transport has remained elusive. For example, the lack of *N*-glycosylation may lead to virtually complete intracellular retention, as has been reported for human vasoactive intestinal peptide 1 and rat AT_{1a} angiotensin II receptors (6, 7). Frequently, however, the expression levels merely decrease, as happens for rat prostaglandin E_2 and human AT_1 receptors (8, 9), or the non-*N*-glycosylated receptors are fully functional and properly localized at the plasma membrane, as is the case for canine histamine H2 and porcine m2 muscarinic acetylcholine receptors (10, 11). Furthermore, these attributes are not necessarily dependent on *N*-glycosylation as such but on a particular *N*-glycan, in a specific position. Bovine rhodopsin has two *N*-glycans positioned in its N termi-

* This work was supported by the Biocenter Oulu and Grant 206230 from the Academy of Finland. The costs of publication of this article were defrayed in part by the payment of page charges. This article must therefore be hereby marked "*advertisement*" in accordance with 18 U.S.C. Section 1734 solely to indicate this fact.

[S] The on-line version of this article (available at http://www.jbc.org) contains supplemental Figs. 1–3.

[1] To whom correspondence should be addressed: Institute of Biomedicine, Dept. of Anatomy and Cell Biology, University of Oulu, P. O. Box 5000, FI-90014, Oulu, Finland. Tel.: 358-8-537-5193; Fax: 358-8-537-5172; E-mail: Ulla.Petaja-Repo@oulu.fi.

[2] The abbreviations used are: ER, endoplasmic reticulum; BSA, bovine serum albumin; δOR, δ-opioid receptor; DMEM, Dulbecco's modified Eagle's medium; Endo H, Endo-β-*N*-acetylglucosaminidase H; FBS, fetal bovine serum; GPCR, G protein-coupled receptor; HEK, human embryonic kidney; NHS, *N*-hydroxysuccinimide; NTX, naltrexone; PBS, phosphate-buffered saline; PE, phycoerythrin; PNGase F, peptide-*N*-glycosidase F; SNC-80, (+)-4-[(α*R*)-α-((2*S*,5*R*)-4-Allyl-2,5-dimethyl-1-piperazinyl)-3-methoxybenzyl]-*N*,*N*-diethylbenzamide; HA, hemagglutinin; hδOR, human δ-opioid receptor; GTPγS, guanosine 5′-3-*O*-(thio)triphosphate.

nus, but only one of them was found to be important for the cell surface expression and function of the receptor (12).

The human δ-opioid receptor (hδOR) is a member of the opioid receptor subfamily that mediates signals of endogenous opioid peptides and exogenous opiate compounds (13). It has been used extensively as a model to investigate GPCR biosynthesis. During its transit from the ER to the plasma membrane, it undergoes extensive modifications, including *N*- and *O*-glycosylation and palmitoylation (14, 15). Its maturation is, however, inefficient (14), and a large fraction of synthesized receptors is degraded in proteasomes (16). The receptors that do not mature are not terminally misfolded but rather represent folding intermediates that are prematurely targeted for degradation. This is suggested by the observation that ER-retained receptors are rescued by opioid receptor pharmacological chaperones, which bind and stabilize newly synthesized receptors and facilitate their transport to the cell surface (17, 18). As the *N*-glycan-mediated quality control is obviously involved in regulating the early steps of hδOR biogenesis, we set out to determine the role of *N*-glycosylation in receptor biosynthesis and function. The two potential *N*-glycosylation sites in its N terminus, Asn^{18} and Asn^{33}, were disrupted, and the mutant receptors were stably expressed in inducible human embryonic kidney 293 (HEK293) cells that express the constructs from the same chromosomal integration site. This provided an efficient tool for accurate quantitative analyses.

EXPERIMENTAL PROCEDURES

Materials—[15,16-^{3}H]Diprenorphine (50.0–54.9 Ci/mmol) and Easytag Express ^{35}S-protein labeling mix (1175 Ci/mmol) were from PerkinElmer Life Sciences. Anti-FLAG M2 and anti-HA (HA-7) monoclonal antibodies, the corresponding antibody affinity resins, and FLAG peptide were obtained from Sigma. The HA peptide was from Innovagen. EZ-linked sulfo-*N*-hydroxysuccinimide (NHS)-biotin and horseradish peroxidase-conjugated streptavidin were from Pierce, and endo-β-*N*-acetylglucosaminidase H (Endo H), peptide-*N*-glycosidase F (PNGase F), *O*-glycosidase, and neuraminidase were purchased from Roche Applied Science. Opioid ligands, naltrexone (NTX), ICI-174,864, SNC-80 ((+)-4-[(α*R*)-α-((2*S*,5*R*)-4-Allyl-2,5-dimethyl-1-piperazinyl)-3-methoxybenzyl]-*N*,*N*-diethylbenzamide), and [Leu^5]enkephalin were obtained from Tocris or Sigma, except for fluorescein-NTX, which was from Invitrogen. Cell culture reagents were purchased from BioWhittaker, Invitrogen, InVivogen, or Sigma. Anti-calnexin (SPA-860) and anti-calreticulin (SPA-600) polyclonal antibodies were purchased from StressGen. Anti-c-Myc (A-14) polyclonal antibody was from Santa Cruz Biotechnology, and anti-c-Myc (9E10) monoclonal antibody was either produced by the core facility at the Department of Biochemistry, University of Montréal, Canada, as ascites fluid or purchased from Santa Cruz Biotechnology. All other reagents were of analytical grade and purchased from various commercial suppliers.

DNA Constructs—The hδOR-pFT-SMMF construct encoding the hδOR (GenBank™ accession number U10504 (56) with a cleavable influenza hemagglutinin signal peptide, N-terminal Myc tag, and C-terminal FLAG-tag has been described previously (18). The hδOR-pcDNA5 encoding the hδOR with a C-terminal FLAG tag was prepared by XhoI/KpnI digestion of the hδOR-FLAG-pcDNA3 (14) and cloning into the pcDNA5 vector (Invitrogen). Preparation of the hδOR-pcDNA5 encoding the hδOR with a hemagglutinin signal peptide and N-terminal HA-tag will be described elsewhere.[3] The wild-type receptor constructs were modified to create the corresponding constructs encoding the N18Q, N33Q, and N18Q/N33Q mutants with QuikChange site-directed mutagenesis kit (Stratagene), using oligonucleotides 5′-CCGCTCTTCGCCGAAGCCTCGGACGCC-3′ and 5′-GGCGTCCGAGGCTTCGGCGAAGAGCGG-3′ to generate the N18Q modification, and 5′-GCGCTGGCGCCGAAGCGTCGGGGCC-3′ and 5′-GGCCCCGACGCTTCGGCGCCAGCGC-3′ to generate the N33Q modification.

Cell Culture and Transfections—The HEK293$_i$-Myc-hδOR-FLAG cell line has been described elsewhere (18, 19). The HEK293$_i$-Myc-hδOR(N18Q)-FLAG, HEK293$_i$-Myc-hδOR(N33Q)-FLAG, and HEK293$_i$-Myc-hδOR(N18Q/N33Q)-FLAG cell lines were created with the same protocol under blasticidin S (4 μg/ml; InVivogen) and hygromycin (400 μg/ml; InVivogen) selection. The stably transfected cells were cultured in Dulbecco's modified Eagle's medium (DMEM), supplemented with 10% (v/v) fetal bovine serum (FBS), 100 units/ml penicillin, and 100 μg/ml streptomycin (complete DMEM). For experiments 0.1, 2, or 5 × 10^6 cells were plated onto 24-well plates or 25- or 75-cm^2 culture flasks, respectively, and cultured for 2 or 3 days to 80% confluency. Receptor expression was induced by supplementing the culture medium with 500 ng/ml tetracycline (Invitrogen) for 24 h, unless otherwise stated. To inhibit export of newly synthesized receptors from the ER (supplemental Fig. 2*D*), brefeldin A (5 μg/ml; Alexis) was added to the medium, and cells were cultured for 6 h in the presence of tetracycline.

Flp-In-293 cells (Invitrogen) were cultured in complete DMEM, supplemented with 100 μg/ml Zeoc (InVivogen), and Flp-In-CHO (Chinese hamster ovarian) cells in F-12 Ham's nutrient mixture with 10% (v/v) FBS, 100 units/ml penicillin, 100 μg/ml streptomycin (complete F-12), supplemented with 100 μg/ml Zeoc. For transient transfections, Flp-In-293 and Flp-In-CHO cells (9 × 10^6 and 4 × 10^6, respectively) were plated onto 100-mm plates and cultured for 24 h. Prior to transfection, the medium was changed to Opti-MEM, supplemented with 4% (v/v) FBS. Lipofectamine 2000 transfection reagent (15 μl, Invitrogen) and constructs (5 μg) were incubated separately in 300 μl of Opti-MEM for 5 min, mixed, and incubated further for 25 min. The mixture was added to the cells, and after 4 h the medium was changed to complete DMEM or Ham's F-12, and cells were harvested 24 h later.

Metabolic Labeling—Cells were pretreated with 500 ng/ml tetracycline for 60 min (Figs. 2, 3, and 5*A*) or 16 h (Fig. 5*B*) in complete DMEM, and the reagent was maintained in the culture medium throughout depletion and labeling. Methionine and cysteine were depleted by incubating cells in methionine- and cysteine-free DMEM for 60 min, and labeling was performed in a fresh medium with 100–200 μCi/ml of [^{35}S]methi-

[3] T.T. Leskelä and U. E. Petäjä-Repo, unpublished data.

onine/cysteine for 30–60 min, as specified in figure legends. The labeling pulse was terminated by washing, and cells were chased in complete DMEM, supplemented with 5 mM methionine, for various periods of time as specified in figures. Inhibitors of lysosomal degradation were added to the chase medium (NH_4Cl 10 mM, chloroquine (Sigma) 0.2 mM, and leupeptin (Alexis) 500 μg/ml), whereas the *N*-glycosylation inhibitor tunicamycin (Alexis) was added 2.5 h before depletion, at a concentration of 5 μg/ml. During depletion and labeling, the tunicamycin concentration was raised to 25 μg/ml. Before harvesting, cells were incubated in phosphate-buffered saline (PBS), supplemented with 20 mM *N*-ethylmaleimide, for 10 min on ice.

Preparation and Solubilization of Membranes and Whole Cell Extracts—Cells were homogenized for radioligand and GTP-binding assays in buffer A (25 mM Tris-HCl, pH 7.4, 5 mM $MgCl_2$, 2 mM EDTA, 5 μg/ml leupeptin, 5 μg/ml soybean trypsin inhibitor, 10 μg/ml benzamidine) and for immunoprecipitation and the heat inactivation assay in buffer B (25 mM Tris-HCl, pH 7.4, 2 mM EDTA, 2 μg/ml aprotinin, 0.5 mM phenylmethylsulfonyl fluoride, 2 mM 1,10-phenanthroline, 5 μg/ml leupeptin, 5 μg/ml soybean trypsin inhibitor, 10 μg/ml benzamidine) as described previously (18). Membranes were resuspended in buffer A for ligand-binding and GTP-binding assays and in buffer B for the heat inactivation assay, at a concentration of 1 mg/ml, and stored at −70 °C. Membranes subjected to immunoprecipitation were suspended in buffer C (buffer B, containing 0.5% (w/v) *n*-dodecyl-β-D-maltoside (Alexis) and 140 mM NaCl) and extracted for 60 min on a magnetic stirrer, and solubilized receptors were separated from the insoluble fraction by centrifugation at 100,000 × *g* for 60 min. Metabolically labeled cells were sonicated with a tip sonicator three times for 15 s in buffer B, and membranes were recovered by centrifugation at 45,000 × *g* for 30 min, washed twice, and extracted in buffer C as above. Total cellular lysates were prepared by suspending frozen cell pellets in buffer C (Figs. 1*E* and 5) or buffer D (buffer C, containing 0.5% (w/v) digitonin (Alexis) and 10 mM $CaCl_2$ but without EDTA; Fig. 3) for 30 min, and the insoluble material was removed by centrifugation at 16,000 × *g* for 30 min. All steps were performed at 4 °C. Protein concentration was determined using DC protein assay kit (Bio-Rad), with bovine serum albumin (BSA) as a standard.

Immunoprecipitation—Solubilized receptors were purified with either one-step (Figs. 1, *B–D,* and 2) or two-step immunoprecipitation (Figs. 1*E* and 5 and supplemental Fig. 1) with the anti-FLAG M2 or anti-HA antibody affinity resin, as described earlier (14, 16), and eluted with 200 μg/ml FLAG or HA peptide, respectively. Alternatively (Fig. 3), cellular lysates were divided into 3 aliquots, supplemented with 0.1% (w/v) BSA, and precleared with 20 μl of protein G-Sepharose (GE Healthcare) for 60 min at 4 °C. One aliquot was subjected to immunoprecipitation with anti-FLAG M2 antibody affinity resin, and the two others were incubated for 60 min at 4 °C with anti-calnexin antibody (1:100) or rabbit preimmune serum (1:100), followed by a 2-h incubation with protein G-Sepharose. Elution was performed with 80 μl of 1% (w/v) SDS in 25 mM Tris-HCl, pH 7.4, by incubating for 15 min at 22 °C and for 5 min at 95 °C. The eluates were diluted with buffer C, supplemented with 0.1% BSA, and immunoprecipitated with anti-FLAG M2 antibody affinity resin as described above.

Deglycosylation of Immunoprecipitated Receptors—Immunoprecipitated receptors were eluted from the anti-FLAG M2 antibody affinity resin with 1% (w/v) SDS, 50 mM sodium phosphate, pH 5.5, by incubating samples for 15 min at 22 °C, and for 5 min at 95 °C. The eluates were diluted 5-fold with buffer E (0.5% (w/v) *n*-dodecyl-β-D-maltoside, 50 mM sodium phosphate, pH 5.5, 4 mM calcium phosphate, 0.5 mM phenylmethylsulfonyl fluoride, 5 μg/ml leupeptin, 5 μg/ml soybean trypsin inhibitor, and 10 μg/ml benzamidine) for *O*-glycosidase and neuraminidase digestions. The enzymes were added to a final concentration of 50 milliunits/ml, and samples were incubated at 30 °C for 16 h before terminating the reaction by adding 40 μl of SDS-sample buffer. Endo H and PNGase F digestions were performed as described (19).

Cell Surface Biotinylation—Receptor expression was induced for 16 h, and cell surface proteins were biotinylated with sulfo-NHS-biotin as described previously (14).

Radioligand Binding Assay—Binding assays were performed using 1–40 μg of membrane protein in a final volume of 300 μl of buffer A, containing 0.1% (w/v) BSA. For saturation binding experiments, triplicate samples were incubated with an increasing concentration of [^{3}H]diprenorphine, the final concentration ranging from 0.01 to 10 nM. For one-point binding assays, each triplicate contained 5 nM [^{3}H]diprenorphine. Nonspecific binding was determined using 10 μM NTX. Samples were harvested, and data were analyzed as described earlier (18).

GTP-binding Assay—To produce cellular membranes with similar low amounts of receptor, cells were induced with 10 ng/ml (hδOR, hδOR(N18Q), and hδOR(N33Q)) or 20 ng/ml (hδOR(N18Q/N33Q)) tetracycline for 24 h. GTP-binding assays were performed using DELFIA GTP-binding kit (PerkinElmer Life Sciences), using a method modified from Frang *et al.* (20). Ten μg of membrane protein was preincubated in a reaction buffer, containing 50 mM HEPES, 5 mM $MgCl_2$, 3 μM GDP, 100 mM NaCl, and 100 μg/ml saponin, in a final volume of 100 μl for 30 min on a plate shaker prior to addition of 10 μl of 100 nM europium-labeled GTP. Receptor activation was induced with 0.01–1000 nM SNC-80, and nonspecific binding was determined by adding 5 μM GTPγS into the reaction buffer. After 30 min, the reaction was terminated by vacuum filtration (Multiscreen Vacuum Manifold, Millipore) and washed twice with ice-cold GTP-Wash Buffer. The bound europium-labeled GTP was measured with VICWallac 1420 VICTOR^2 Multilabel microplate reader, using the europium measurement protocol (excitation 350 nm, emission 615 nm, 0.4 ms delay, 0.4-ms window).

Analysis of Cell Surface Receptor Expression by Flow Cytometry—The total pool of cell surface receptors was labeled with anti-c-Myc antibody (9E10, ascites fluid 1:500) or anti-HA antibody (HA-7, 1:500) and phycoerythrin (PE)-conjugated rat anti-mouse IgG_1 (BD Biosciences, 1 μg/ml) as described earlier (15). Fluorescein-NTX was used to label the ligand binding competent pool of cell surface receptors (Table 2 and supplemental Fig. 2). For this assay, cells were labeled directly on cell culture plates in the dark at 22 °C for 0–60 min, in the presence

of the conjugated ligand in a final concentration of 0.1 nM to 10 μM and in the presence or absence of 10 μM NTX or ICI-174,864 in PBS, 1% (v/v) FBS (PBS/FBS). Dead cells were labeled with 0.25 μg/ml 7-amino-actinomycin D (BD Biosciences) in PBS/FBS for 10 min in the dark on ice. Cells were detached, washed, and resuspended in PBS/FBS, and 10,000 cells of each sample were analyzed on BD Biosciences FACSCalibur flow cytometer, exciting cells with 488-nm argon ion laser. The fluorescein, PE, and 7-amino-actinomycin D emissions were detected with 530 ± 15-, 585 ± 21-, and 670-nm long-pass filters, respectively. Data were analyzed with CellQuestPro 4.02 software (BD Biosciences), and the mean fluorescence of live induced cells minus the mean fluorescence of live noninduced cells was used for calculations.

Quantitation of Receptor Internalization by Flow Cytometry—For assessing constitutive internalization, cell surface receptors were labeled with anti-c-Myc antibody (9E10, 2 μg/ml; Santa Cruz Biotechnology) in complete DMEM for 30 min at 37 °C. Cells were then thoroughly washed and chased in the medium for up to 4 h at 37 °C, washed again with cold PBS, and labeled with PE-conjugated secondary antibody (1 μg/ml) in PBS/FBS on ice. Agonist-induced internalization was initiated by supplementing the culture medium with 1 μM Leu-enkephalin, and incubating cells at 37 °C for up to 60 min. Cells were washed with ice-cold PBS, and cell surface receptors were labeled with anti-c-Myc antibody (2 μg/ml; Santa Cruz Biotechnology) and PE-conjugated secondary antibody (1 μg/ml) in PBS/FBS on ice. For all internalization assays, dead cells were labeled with 7-amino-actinomycin D, and triplicate samples of 10,000 cells were analyzed as described above.

Heat Inactivation Assay—Cellular membranes (200 μg of protein) were incubated in Eppendorf Thermomixer (650 rpm) at 37 °C for different periods of time as indicated in supplemental Fig. 3. After terminating the incubations by placing the samples on ice, membranes were diluted to 100–150 μg/ml, and $MgCl_2$ concentration was adjusted to 5 mM. The one-point binding assay was performed using 100 μl of the suspension and a saturating concentration of [^{3}H]diprenorphine (5 nM) as described above.

Confocal Microscopy—Cells were cultured on poly-L-lysine (100 μg/ml)-coated coverslips, and receptor expression was induced with 500 ng/ml tetracycline for 7 h, after which cells were fixed with 2% (w/v) of paraformaldehyde for 15 min at 22 °C. To inhibit lysosomal degradation, leupeptin (500 μg/ml) was added into the culture medium 60 min after initiating the induction. Two hours later the medium was supplemented with either anti-c-Myc (A-14, 2 μg/ml) or anti-FLAG M2 (2.5 μg/ml) antibodies or the lysosomal marker LysoTrackerRed DND-99 (200 nM, Invitrogen) or in combination. Fixed cells were permeabilized with 0.1% (v/v) Triton X-100, 0.5% (w/v) BSA, PBS for 45 min. After washing with PBS, cells were incubated with primary antibodies (anti-FLAG M2 antibody (10 μg/ml) or anti-calreticulin antibody (1:1000) in the permeabilization buffer, 30 min), and with secondary antibodies (Alexa Fluor 488 goat anti-mouse/anti-rabbit (1:200) and Alexa Fluor 568 goat anti-mouse/anti-rabbit (1:200) (Invitrogen) in the permeabilization buffer, 30 min). After final washes with PBS, coverslips were mounted on glass slides with Immu-mount (ThermoElectron) for confocal microscopy. Immunofluorescence staining was viewed with Zeiss LSM510 confocal microscope, using Zeiss Plan-Apo 100 × 1.4 NA oil immersion objective under the 488- and 647-nm wavelength excitation.

SDS-PAGE, Fluorography, and Western Blotting—Protein samples were reduced in the presence of 50 mM dithiothreitol, incubated for 2 min at 95 °C for complete denaturation, and analyzed in 10% SDS-polyacrylamide gels, using reagents from Bio-Rad or Amresco. Western blotting as well as fluorography, densitometric scanning, and data analysis for the detection and analysis of radioactively labeled proteins were performed as described previously (18, 21). Films were scanned with Umax PowerLook 1120 color scanner and Image Master 2D Platinum 6.0 software.

Data Analysis—Data were analyzed using GraphPad Prism 4.02 software. Statistical analyses were performed using the regression analysis or analysis of variance with post-test Tukey analysis for experiments with more than one variable. Student's *t* test was performed for experiments with one variable only. The limit of significance was set at $p < 0.05$, and the data are presented as mean ± S.E.

RESULTS

hδOR Carries Two N-Linked Glycans, Both of Which Are Dispensable for Receptor Cell Surface Expression—The hδOR contains two putative consensus sequences for *N*-linked glycosylation (Asn^{18}-Ala-Ser and Asn^{33}-Ala-Ser) at its N terminus (Fig. 1*A*). To determine whether both sites are occupied, and to study the effect of *N*-glycosylation on hδOR processing and trafficking, the asparagine residues were mutated to glutamines by modifying the hδOR construct that encodes the receptor with a cleavable hemagglutinin signal sequence (22) and Myc and FLAG epitopes at the N and C termini, respectively (18) (Fig. 1*A*). The modified receptor constructs (hδOR(N18Q), hδOR(N33Q), and hδOR(N18Q/N33Q)) were stably transfected into a HEK293$_i$ cell line (18, 19) that allowed expression of all constructs from the same chromosomal integration site.

To identify the receptor species that were expressed, the stably transfected HEK293$_i$ cells were treated with or without 500 ng/ml tetracycline for 24 h to induce receptor expression, and receptors were immunoprecipitated from solubilized membranes with immobilized anti-FLAG M2 antibody and analyzed by SDS-PAGE and Western blotting. All four cell lines displayed unique patterns of receptor species, but only under tetracycline induction (Fig. 1*B*). As we have shown previously (18, 23), one major species of M_r 61,000 and two minor ones of M_r 47,000 and M_r 51,000 were immunoprecipitated from induced cells that were transfected with the wild-type receptor construct (Fig. 1*B*, *lane 2*). The smallest receptor species of M_r 47,000 was sensitive to Endo H digestion (Fig. 1*C*, *lane 2*), indicating that it represents the receptor precursor. In contrast, the two larger ones were Endo H-resistant but were digested with PNGase F (Fig. 1*C*, *lanes 2* and *3*, respectively), thus corresponding to mature receptor forms carrying complex-type *N*-glycans. When Asn^{18} was mutated to glutamine, the immunoprecipitated receptor migrated as two species of M_r 44,000 and M_r 52,000 (Fig. 1*B*, *lane 4*), both of which were sensitive to PNGase F (Fig. 1*C*, *lane 6*). Two PNGase F-sensitive receptor

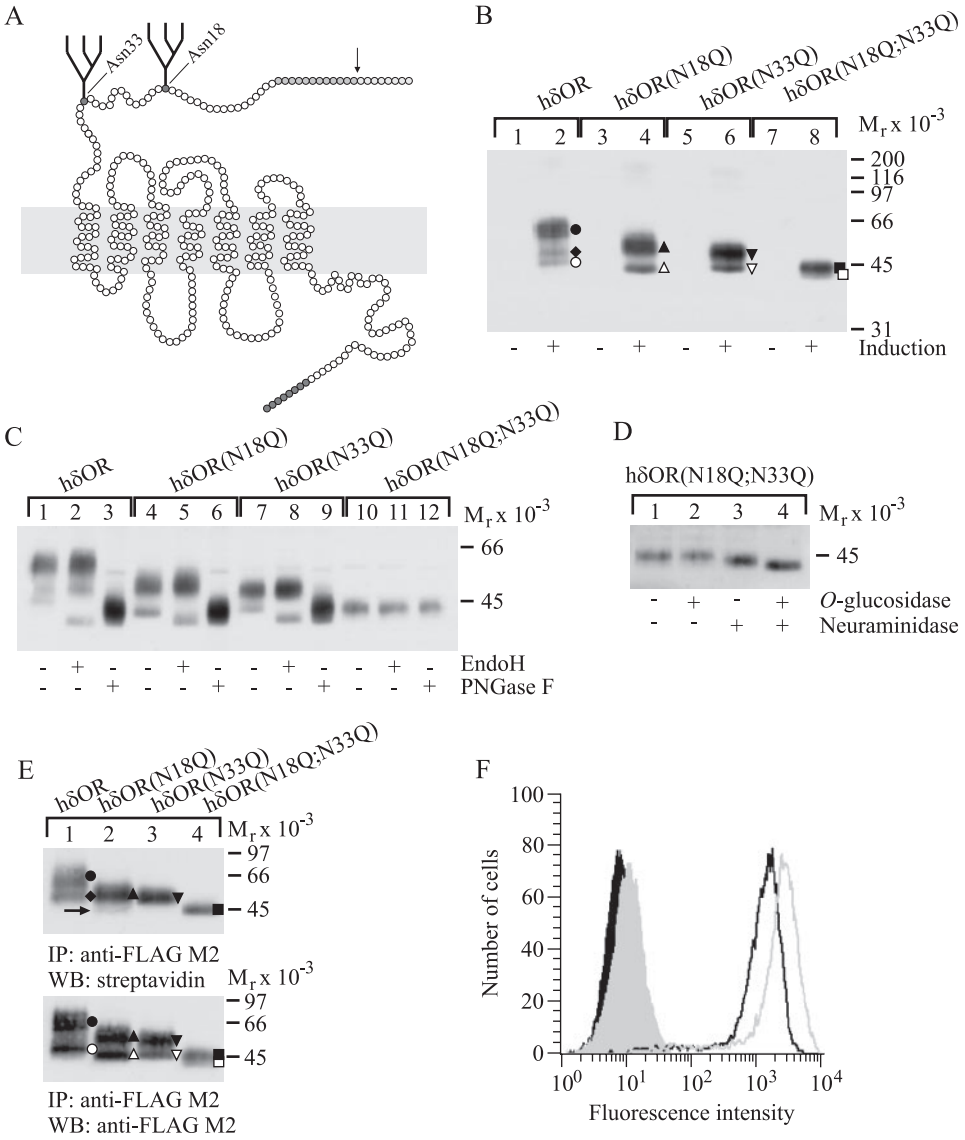

FIGURE 1. **The hδOR contains two *N*-linked glycans and both are dispensable for receptor cell surface expression.** *A*, topography of the hδOR. The two *N*-glycosylation sites at the receptor N terminus are indicated. The N-terminal Myc and C-terminal FLAG epitope tags are shown in *light* and *dark gray*, respectively. The cleavable hemagglutinin signal sequence is also shown. *B,* HEK293$_i$ cells expressing the wild-type hδOR (*lanes 1* and *2*) or the N18Q (*lanes 3* and *4*), N33Q (*lanes 5* and *6*), or N18Q/N33Q (*lanes 7* and *8*) mutants were induced or not for 24 h. Expressed receptors were immunoprecipitated from solubilized membranes with anti-FLAG M2 antibody and analyzed by Western blotting with the same antibody. *C,* immunoprecipitated receptors were deglycosylated at 30 °C for 16 h with 50 milliunits/ml Endo H or 50 units/ml PNGase F, and analyzed as described for *B*. *D,* immunoprecipitated hδOR(N18Q/N33Q) was treated with 50 milliunits/ml *O*-glycosidase (*lane 2*), 50 milliunits/ml neuraminidase (*lane 3*), or with both enzymes simultaneously (*lane 4*) at 30 °C for 16 h, and analyzed as described for *B*. *E,* HEK293$_i$ cells expressing the wild-type hδOR (*lane 1*) or the N18Q (*lane 2*), N33Q (*lane 3*), or N18Q/N33Q (*lane 4*) mutants were induced for 16 h, and cell surface proteins were labeled with 500 ng/ml sulfo-NHS-biotin for 30 min on ice. Receptors were purified from cell lysates as described for *B* and analyzed by Western blotting using either horseradish peroxidase-conjugated streptavidin (*upper panel*) or anti-FLAG M2 antibody (*lower panel*). Molecular weight markers used to calibrate the gels are indicated on the *right*. The precursor and mature receptor forms are indicated with *open* and *closed symbols*, respectively. ○ and ●, wild-type hδOR; △ and ▲, hδOR(N18Q); ▽ and ▼, hδOR(N33Q); □ and ■, hδOR(N18Q/N33Q). For the wild-type receptor, two mature receptor species were detected, carrying either one or two *N*-glycans (◆ and ●, respectively). The *arrow* on *lane 2* of the *upper E* points to a non-*N*-glycosylated receptor that was occasionally detected for the hδOR(N18Q). *IP*, immunoprecipitation; *WB,* Western blotting. *F,* HEK293$_i$ cells expressing the wild-type hδOR (*gray*) or the N18Q/N33Q (*black*) mutant were induced for 24 h, and cells surface receptors were labeled with anti-c-Myc antibody, followed by PE-conjugated secondary antibody. The fluorescence intensity of live cells was measured by flow cytometry. The *shaded curves* represent the background signal obtained in the absence of the primary antibody.

forms of M_r 45,000 and M_r 51,000 were also detected when Asn^{33} was mutated to glutamine (Fig. 1, *B*, *lane 6*, and *C*, *lane 9*). The smaller molecular weight mutant receptor forms represent receptor precursors, as they were digested with Endo H (Fig. 1*C*, *lanes 5* and *8*). These results clearly indicate that both *N*-glycosylation sites of the hδOR are used. The differences in the electrophoretic mobility of the mature mutant receptor forms (compare *lanes 4* and *6* in Fig. 1*B*) indicate that the two *N*-glycans are processed in a dissimilar manner in the Golgi and/or otherwise have a different effect on electrophoretic mobility of the receptor. In addition, because the smaller Endo H-resistant wild-type receptor form co-migrated with the Endo H-resistant hδOR(N33Q) mutant (compare *lanes 2* and *6* in Fig. 1*B*), the M_r 51,000 wild-type receptor is likely to correspond to a species that carries only one *N*-glycan at Asn^{18}.

When both Asn^{18} and Asn^{33} of the hδOR were mutated, the double mutant migrated as a single M_r 45,000 species on SDS-PAGE (Fig. 1*B*, *lane 8*). Occasionally an ill-defined species migrating slightly faster than the M_r 45,000 one was also apparent. As expected, the M_r 45,000 species was insensitive to both Endo H and PNGase F (Fig. 1*C*, *lanes 11* and *12*, respectively). However, its molecular weight was higher than that of the deglycosylated precursors of the wild-type receptor or single mutants (Fig. 1*C*, compare *lane 10* to *lanes 2, 5,* and *8*), suggesting that it contains other post-translational modifications. As the hδOR has been shown to undergo *O*-glycosylation (14), we tested the possibility that the M_r 45,000 receptor form might also contain *O*-glycans by subjecting the immunoprecipitated receptor to glycosidase digestions. As seen in Fig. 1*D*, the hδOR(N18Q/N33Q) was sensitive to *O*-glycosidase, but only if the samples were treated simultaneously with neuraminidase. This points out that the M_r 45,000 receptor species represents a receptor form that is devoid of *N*-glycans but contains sialylated *O*-glycans.

O-Glycosylation of the hδOR is known to take place in the Golgi (14), suggesting that the M_r 45,000 form of the hδOR(N18Q/N33Q) represents a receptor species that has

TABLE 1

Ligand binding and G protein-coupling properties of wild-type and mutant hδORs

Ligand- and GTP-binding assays were carried out using membranes that were prepared from stably transfected HEK293$_i$ cells, expressing the wild-type hδOR or the N18Q, N33Q, or N18Q/N33Q mutants. Cells were treated for 24 h with 500 ng/ml tetracycline for the ligand-binding assays or with either 10 ng/ml (hδOR, hδOR(N18Q), hδOR(N33Q)) or 20 ng/ml (hδOR(N18Q/N33Q)) tetracycline for the GTP-binding assays. Saturation binding assays were performed using 0.01–10 nM [^{3}H]diprenorphine to obtain the K_d and B_{max} values. The GTP-binding assays were carried out using 0.01–1000 nM SNC-80 to obtain the EC_{50} and E_{max} values. The receptor densities in membranes used for the GTP-binding assays were measured by a one-point binding assay using 5 nM [^{3}H]diprenorphine, and the values were 2.9 ± 0.6, 2.7 ± 0.5, 2.9 ± 0.3, and 2.6 ± 0.6 pmol/mg protein for the wild-type hδOR, hδOR(N18Q), hδOR(N33Q), and hδOR(N18Q/N33Q), respectively. Analysis of the data was performed using GraphPad Prism. Data represent the mean ± S.E. of three independent experiments, performed in triplicate.

Receptor	Ligand binding [^{3}H]Diprenorphine		GTP binding, SNC-80		
	K_d [a]	B_{max} [b]	Basal	E_{max} [c]	EC_{50} [d]
	nM	*pmol/mg protein*	*cps/10 μg protein*	*% over basal*	*nM*
hδOR	1.52 ± 0.39	59.5 ± 4.8	3752 ± 539	174 ± 6	12.6 ± 1.8
hδOR(N18Q)	1.34 ± 0.19	41.5 ± 2.4[e]	3126 ± 75	192 ± 49	18.2 ± 2.6
hδOR(N33Q)	1.57 ± 0.34	36.7 ± 3.0[e]	3590 ± 357	222 ± 35	21.5 ± 4.2
hδOR(N18Q/N33Q)	1.27 ± 0.38	21.6 ± 3.6[e]	3044 ± 151	242 ± 17	24.1 ± 3.2[f]

[a] Equilibrium dissociation constant is indicated.
[b] Maximal specific binding is indicated.
[c] Maximal stimulation is indicated.
[d] Half-maximal effective concentration is indicated.
[e] $p < 0.001$.
[f] $p < 0.05$ is compared with the wild-type hδOR, using Tukey's post test after analysis of variance test.

been exported from the ER. To further confirm that the M_r 45,000 non-*N*-glycosylated receptor is indeed able to reach the plasma membrane, cell surface proteins were labeled with membrane-impermeable sulfo-NHS-biotin. The immunoprecipitated receptors were then analyzed by Western blotting, using either horseradish peroxidase-conjugated streptavidin or anti-FLAG M2 antibody. As expected, streptavidin was only able to detect the Endo H-resistant forms of the wild-type receptor and single mutants, whereas the antibody detected all receptor forms (Fig. 1*E*, compare *lanes 1–3* in the *upper* and *lower panels*). Streptavidin was also able to detect the immunoprecipitated M_r 45,000 hδOR(N18Q/N33Q) species but not the ill-defined M_r 42,000 one (Fig. 1*E*, *lane 4*), indicating that the latter represents an intracellular form of the double mutant. Importantly, this intracellular form of the non-*N*-glycosylated receptor was relatively less abundant than that of the other receptor constructs. The same appeared to apply also to the cell surface form (Fig. 1*E*, compare *lanes 1–4* in the *lower panel*). The lower cell surface expression level of the non-*N*-glycosylated receptor was confirmed by flow cytometry, using anti-c-Myc antibody and PE-conjugated secondary antibody (Fig. 1*F*, see also Table 2). Similar results were also obtained by transient transfection of Flp-In-293 and Flp-In-CHO cells with constructs encoding the wild-type hδOR and the N18Q/N33Q mutant with Myc, HA, or FLAG epitope tags (supplemental Fig. 1).

N-Glycans of the hδOR Are Not Essential for Receptor Function—To assess the effect of *N*-glycosylation on the ligand-binding ability of the hδOR, crude cellular membranes from induced stably transfected HEK293$_i$ cells were subjected to saturation binding assays, using the opioid antagonist [^{3}H]diprenorphine as a radioligand. As seen in Table 1, the maximal binding capacity (B_{max}) measured for the wild-type receptor expressing cells was significantly higher than for the receptor mutant cell lines. The lowest expression level was measured for the non-*N*-glycosylated receptor, with a B_{max} of only 36% of the wild-type receptor level. However, the affinities for the ligand were similar for all receptors and were comparable with values reported previously for the wild-type receptor (24), thus indicating that the hδOR does not need *N*-glycans for ligand binding.

The effect of *N*-glycosylation on downstream signaling of the hδOR was examined by measuring stimulation of nucleotide exchange at heterotrimeric G proteins. The ability of increasing concentrations of SNC-80, a δOR-specific agonist, to stimulate GTP binding to G proteins was assessed for cellular membranes prepared from stably transfected HEK293$_i$ cells that were induced with low concentrations of tetracycline. This was necessary to obtain sufficiently low and comparable amounts of receptor expression and to avoid saturation of the reaction components (~2–4 pmol/mg of membrane protein). There were no differences in the basal stimulation, and the agonist induced about 2-fold increase in GTP binding for all receptor constructs. The potency of SNC-80 was, however, decreased by 1.9-fold for the non-*N*-glycosylated receptor (Table 1).

Non-N-glycosylated hδORs Mature Faster and Have a Shorter Half-life than the Wild-type Receptor—The findings that the non-*N*-glycosylated hδOR existed mainly in the mature cell surface form but was expressed at a much lower level than the wild-type receptor suggest that *N*-linked glycosylation may have a role in receptor maturation and/or turnover. Thus, to investigate these possibilities further, metabolic pulse-chase labeling experiments were performed. Receptor expression was induced for 2 h, and methionine-depleted cells were labeled with [^{35}S]methionine/cysteine and chased for various periods of time. At each time point, cells were harvested, and solubilized membrane extracts were subjected to immunoprecipitation with anti-FLAG M2 antibody and immunoprecipitated receptors were analyzed by SDS-PAGE and fluorography. As seen in Fig. 2*A*, two receptor forms of M_r 47,000 and M_r 44,000 were detected for the wild-type receptor at the end of the pulse (*lane 1*). In time, these receptor forms, which were both Endo H-sensitive (data not shown), started to disappear, and two higher molecular weight forms of M_r 61,000 and M_r 51,000 started to accumulate (Fig. 2*A*, *lanes 2–6*). These results confirm that the wild-type receptor exists in two glycoforms, containing either one or two *N*-glycans, the latter one being the predominant species. In line with this notion, only one low

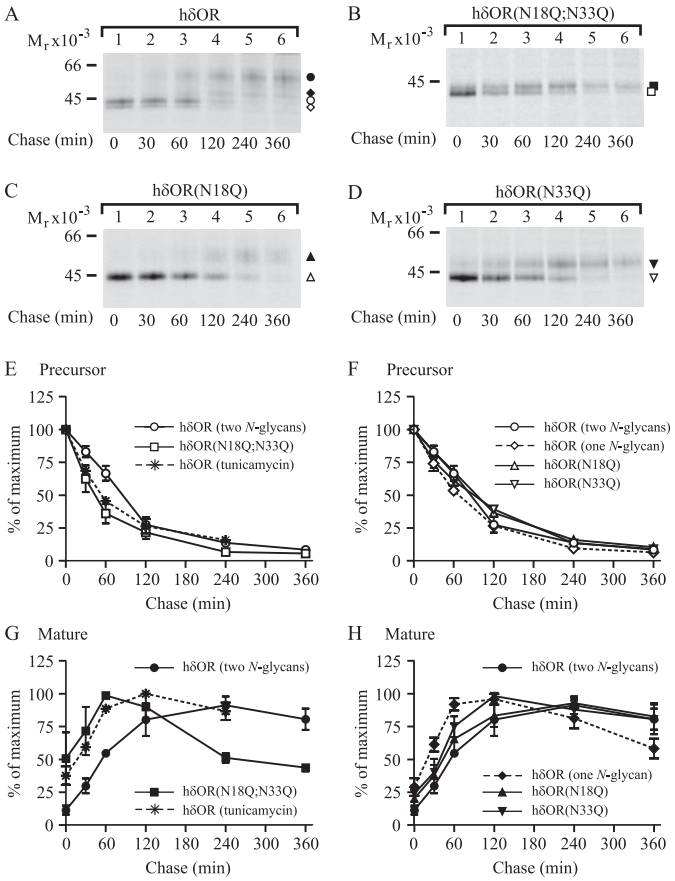

FIGURE 2. **Analysis of hδOR maturation by metabolic pulse-chase labeling.** HEK293$_i$ cells expressing the wild-type hδOR (*A*) or the N18Q (*C*), N33Q (*D*), or N18Q/N33Q (*B*) mutants were induced to express the receptor for 2 h, pulse-labeled with 100–150 μCi/ml [^{35}S]methionine/cysteine for 30–60 min, and chased for the indicated periods of time. Alternatively, cells expressing the wild-type hδOR were treated with tunicamycin to inhibit *N*-glycosylation (5 μg/ml 2.5 h prior to labeling and 25 μg/ml during depletion, labeling, and chase). Receptors were immunoprecipitated with anti-FLAG M2 antibody from solubilized membranes and analyzed by SDS-PAGE and fluorography. *E* and *F* describe the time course of disappearance of the labeled receptor precursors, and *G* and *H* describe appearance of mature forms of the receptor, respectively, analyzed with GraphPad Prism. Intensities of the labeled receptor species were obtained by densitometric scanning of fluorograms, and the values were normalized to the labeled receptor precursor at the beginning of the chase (*E* and *F*) or to the maximum labeling of the mature receptor during the chase (*G* and *H*). The values given are means ± S.E. of three to four independent experiments. The precursor and mature receptor forms are indicated with *open* and *closed symbols*, respectively. ○ and ●, wild-type hδOR carrying two *N*-glycans; ◇ and ◆, wild-type hδOR carrying one *N*-glycan; △ and ▲, hδOR(N18Q); ▽ and ▼, hδOR(N33Q); □ and ■, hδOR(N18Q/N33Q); *, wild-type hδOR, treated with tunicamycin.

molecular weight Endo-H-sensitive receptor species was detected for the single mutants, the hδOR(N18Q) and hδOR(N33Q) (Fig. 2, *C* and *D*, *lane 1*, respectively). In contrast, two low molecular weight receptor species were detected for the double mutant at the end of the pulse (Fig. 2*B*, *lane 1*). As the smaller one disappeared in time, it represents the precursor form of the non-*N*-glycosylated receptor that was barely detectable by Western blotting (see Fig. 1*B*, *lane 8*).

Precursors of the wild-type receptor and the N18Q mutant were converted to the mature form with similar overall kinetics, reaching completion within 4 h (Fig. 2*H*). The N33Q mutant, on the other hand, displayed somewhat enhanced kinetics of maturation that was complete already within 2 h (Fig. 2*H*). Interestingly, faster maturation kinetics appeared to characterize also the wild-type receptor that carried only one *N*-glycan (Fig. 2*H*). This is in line with the notion that the carbohydrate is attached to Asn^{18} in the one *N*-glycan form. The differences in the maturation kinetics were not reflected in the maturation efficiency. It varied from 20 to 60% for both the wild-type receptor and the N18Q and N33Q mutants.

In contrast to what was observed for the single mutants (Fig. 2*F*), the precursor of the double mutant disappeared significantly faster than that of the wild-type receptor (half-time for disappearance 43 ± 4 and 76 ± 10 min for the hδOR(N18Q/N33Q) and wild-type hδOR, respectively, $p < 0.05$) (Fig. 2*E*). Furthermore, a substantial amount of the non-*N*-glycosylated receptor was in the mature form already at the beginning of the chase (Fig. 2*B*, *lane 1*), and the half-time for maturation was significantly shortened (42 ± 9 and 110 ± 9 min for the hδOR(N18Q/N33Q) and wild-type hδOR, respectively, $p < 0.001$) (Fig. 2*G*). In addition, the mature non-*N*-glycosylated receptor started to disappear after 2 h, and less than half of the receptors were apparent after 6 h (Fig. 2*G*). This was in contrast to receptors that carried the *N*-glycan at Asn^{33}. They were more stable, and their amount started to disappear only after 4 h (Fig. 2*H*).

To confirm that the distinct changes in the maturation of the hδOR(N18Q/N33Q) did not result from the replacement of the two asparagines in the receptor N terminus, pulse-chase labeling experiments were conducted using wild-type receptor expressing cells that were treated with tunicamycin, which inhibits co-translational addition of core *N*-glycans to glycoproteins (25). As expected, the receptor precursors disappeared faster in these cells (Fig. 2*E*), and the maturation kinetics was enhanced (Fig. 2*G*).

hδORs Carrying Either One or Two N-Glycans Interact with Calnexin—The results of the pulse-chase labeling experiments indicate that the non-*N*-glycosylated hδOR is exported from the ER faster than receptors carrying either one or two *N*-glycans. Because the ER lectins calnexin and calreticulin are known to be involved in the quality control and retention of glycoproteins in the ER (1), it can be hypothesized that the enhanced ER export might be due to the absence of interaction with these ER chaperones. We therefore tested the ability of the different receptor constructs to associate with calnexin by sequential co-immunoprecipitation. Stably transfected HEK293$_i$ cells that were induced to express the different receptors were labeled with [^{35}S]methionine/cysteine for 30 min, and cellular lysates were prepared. The total pool of receptors was purified by two-step immunoprecipitation using anti-FLAG M2 antibody, and the calnexin-interacting receptor pool was recovered from the denatured anti-calnexin immunoprecipitate by second immunoprecipitation with anti-FLAG M2 antibody. As we have previously reported (18, 23), the wild-type receptor precursor was readily recovered from the calnexin immunoprecipitate, whereas only a trace amount of the non-*N*-glycosylated receptor was recovered (Fig. 3*B*, *lanes 1* and *4*, respectively). If the calnexin antibody was replaced with preimmune serum, no wild-type receptor precursor was detected (Fig. 3*C*, *lane 1*), confirming the specificity of the observed interaction. The precursors of the two single mutants were also

recovered from the calnexin immunoprecipitate, but only about half of the receptors were actually recovered (compare *lanes 2* and *3* in Fig. 3, *A* and *B*). In comparison, hardly any of the wild-type receptor precursors carrying one *N*-glycan were immunoprecipitated with calnexin (Fig. 3*B*, *lane 1*), although they were quite abundant in the anti-FLAG M2 antibody immunoprecipitate (Fig. 3*A*, *lane 1*).

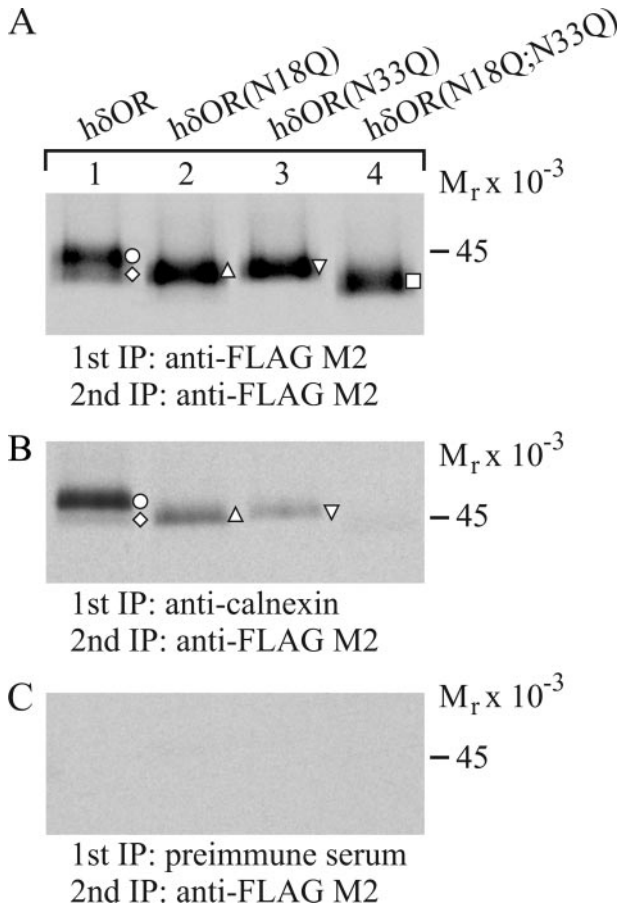

FIGURE 3. **Both *N*-linked glycans of the hδOR are required for the efficient calnexin interaction.** HEK293$_i$ cells expressing the wild-type hδOR or the N18Q, N33Q, or N18Q/N33Q mutants (*lanes 1–4*, respectively) were induced to express the receptor for 2 h, pulse-labeled with 200 μCi/ml [^{35}S]methionine/cysteine for 30 min, and harvested. Cellular lysates were divided into equal aliquots and subjected to immunoprecipitation with anti-FLAG M2 (*A*) or anti-calnexin (*B*) antibodies or preimmune serum (*C*), and receptors were recovered from the denatured eluates by second immunoprecipitation with anti-FLAG M2 antibody. The final eluates were analyzed by SDS-PAGE and fluorography. The receptor precursor forms are indicated with *open symbols*. ○ and ◇, wild-type hδOR carrying two or one *N*-glycans, respectively; △, hδOR(N18Q); ▽, hδOR(N33Q); □, hδOR(N18Q/N33Q). *IP*, immunoprecipitation.

Part of the Non-N-glycosylated hδORs at the Cell Surface Are Incapable of Ligand Binding—As was shown by the cell surface biotinylation assay and flow cytometry and suggested by the pulse-chase labeling experiments, the hδORs are transported to the cell surface whether the receptor molecules are *N*-glycosylated or not. However, it can be hypothesized that the enhanced maturation kinetics of the non-*N*-glycosylated receptors, and their significantly decreased ability to exploit the ER quality control machinery, may result in defective folding. Therefore, we wanted to assess the cell surface receptor population in more detail by flow cytometry, using both antibodies and fluorescein-conjugated opioid antagonist NTX. The ability of the conjugated antagonist to bind to cell surface receptors was first validated by control experiments, assessing the ligand binding conditions and specificity, and ascertaining the membrane nonpermeable nature of the ligand (supplemental Fig. 2).

For the flow cytometry assays, the induced stably transfected HEK293$_i$ cells were labeled with fluorescein-NTX (0.1 μM) or anti-c-Myc antibody, followed by PE-conjugated secondary antibody. In agreement with the saturation ligand-binding assays, less cell surface fluorescence was detected for cells expressing the mutant receptors, whether the labeling was carried out with the antibody or the conjugated ligand (Table 2), the difference reaching a significant level for the hδOR(N33Q) and hδOR(N18Q/N33Q). Importantly, the non-*N*-glycosylated receptor appeared to bind less ligand than expected, as the ratio of the ligand binding pool and the total pool of receptors for the hδOR(N18Q/N33Q) was only 77% that for the wild-type receptor. This suggests that a substantial fraction of the non-*N*-glycosylated receptor population at the plasma membrane is in a conformation that is incompatible with ligand binding.

Non-N-glycosylated hδORs Are More Prone to Internalization with or without Agonist-mediated Activation—As the turnover of mature non-N-glycosylated receptors was increased (see Fig. 2*G*), it is likely that they are internalized and targeted for degradation more extensively than the wild-type receptors. To investigate this further, receptor internalization was followed by flow cytometry. To study constitutive internalization, the stably transfected HEK293$_i$ cells expressing the wild-type hδOR and the N18Q/N33Q mutant were induced, plasma membrane receptors were labeled with anti-c-Myc antibody, and the remaining antibody-bound receptors at the cell surface were

TABLE 2

Cell surface expression of wild-type and mutant hδORs

Stably transfected HEK293$_i$ cells expressing the wild-type hδOR or the N18Q, N33Q, or N18Q/N33Q mutants were induced for 24 h. Cells were labeled with anti-c-Myc antibody (9E10), followed by PE-conjugated secondary antibody, or with 0.1 μM fluorescein-NTX, and the fluorescence of live cells was measured with flow cytometry. The GeoMean values were normalized to those obtained for the wild-type hδOR that were set to 100%. The data were obtained from three independent experiments, performed in duplicate, and analyzed with CellQuest Pro and GraphPad Prism.

Receptor	Total receptor level, anti-c-Myc antibody staining		Ligand-binding competent receptor level, fluorescein-NTX staining		Ratio of ligand binding competent and total receptor levels, fluorescein-NTX/anti-c-Myc antibody	
	GeoMean	% of wild-type hδOR	GeoMean	% of wild-type hδOR	Ratio	% of wild-type hδOR
hδOR	1781 ± 133	100.0	751 ± 23	100.0	0.42 ± 0.01	100.0
hδOR(N18Q)	1617 ± 247	89.9 ± 7.0	682 ± 33	90.9 ± 3.9	0.42 ± 0.02	100.0 ± 4.8
hδOR(N33Q)	1422 ± 186[a]	79.2 ± 4.4	602 ± 54[a]	80.2 ± 6.9	0.42 ± 0.04	100.5 ± 9.0
hδOR(N18Q/N33Q)	1150 ± 145[b]	64.1 ± 3.3	375 ± 18[b]	49.9 ± 2.0	0.33 ± 0.02[a]	77.3 ± 3.8

[a] $p < 0.05$.
[b] $p < 0.001$ is compared with the wild-type hδOR, using Tukey's post test after analysis of variance test.

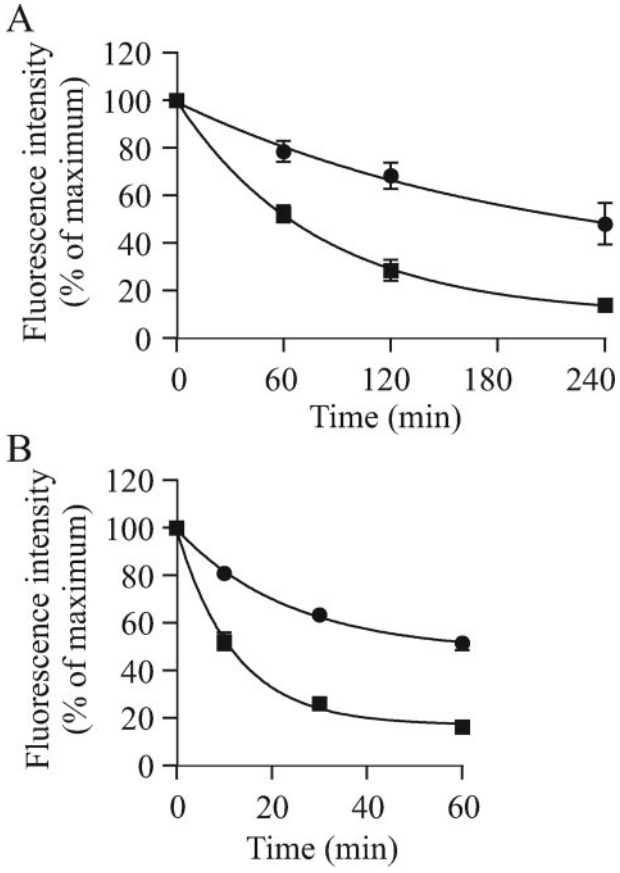

FIGURE 4. **Non-*N*-glycosylated hδORs are internalized faster from the cell surface than wild-type hδORs.** *A*, constitutive internalization. HEK293$_i$ cells expressing the wild-type hδOR or the N18Q/N33Q mutant were induced for 24 h, and cell surface receptors were labeled at 37 °C for 30 min with anti-c-Myc antibody (9E10). After washing, cells were chased for the indicated periods of time at 37 °C, and the remaining antibody-labeled receptors at the cell surface were stained with PE-conjugated secondary antibody and analyzed by flow cytometry. *B*, agonist-induced internalization. HEK293$_i$ cells expressing the wild-type hδOR or the N18Q/N33Q mutant were induced for 24 h and incubated in the presence of 1 μM Leu-enkephalin at 37 °C for the indicated periods of time. Receptors remaining at the cell surface were labeled with monoclonal anti-c-Myc antibody (9E10) on ice for 30 min, followed by PE-conjugated secondary antibody, and analyzed by flow cytometry. The GeoMean values were analyzed with CellQuest Pro and GraphPad Prism, and the values shown are means ± S.E. of three independent experiments, performed in triplicate. The values were normalized to those obtained at the beginning of the incubation. ●, wild-type hδOR; ■, hδOR(N18Q/N33Q).

labeled with PE-conjugated secondary antibody after a chase. As seen in Fig. 4*A*, internalization occurred for both receptors and, as expected, was more pronounced for the non-*N*-glycosylated receptor, affecting significantly the level of cell surface receptors remaining after 4 h (48 ± 9 and 14 ± 1% for wild-type hδOR and hδOR(N18Q/N33Q), respectively; $p < 0.05$). In addition, the mutant receptors internalized faster (half-time for internalization was about 55 and 140 min for the mutant and wild-type receptors, respectively). A similar difference between the two receptors was also detected following agonist-mediated activation (Fig. 4*B*), when cells were treated with an opioid agonist Leu-enkephalin (1 μM), and the remaining cell surface receptors were labeled after 10, 30, or 60 min with anti-c-Myc antibody and PE-conjugated secondary antibody. Within 60 min, 52 ± 3 and 84 ± 1% ($p < 0.05$) of the wild-type and non-*N*-glycosylated receptors, respectively, were internalized (Fig. 4*B*).

As the agonist-mediated internalization concerns receptors that are able to bind ligand, we next tested the possibility that the ligand binding competent mutant receptors might be structurally more unstable than the corresponding wild-type ones. For this purpose, a heat inactivation assay was applied that has been widely used to assess the structural instability of GPCRs (18, 26). Cellular membranes from HEK293$_i$ cells that were induced to express the wild-type hδOR or hδOR(N18Q/N33Q) were incubated at 37 °C for increasing periods of time, and the remaining ligand-binding ability was tested using [^{3}H]diprenorphine. The binding ability of both receptors decreased in time, and the inactivation for the non-*N*-glycosylated receptor appeared to be faster at early time points (supplemental Fig. 3). However, the differences were minor, and the remaining ligand-binding ability was similar at the end of the 60-min incubation.

Non-N-glycosylated hδORs Are Targeted for Lysosomal Degradation—Lysosomal targeting of internalized hδORs was then investigated. First, metabolic pulse-chase labeling experiments were performed using the hδOR(N18Q/N33Q) expressing HEK293$_i$ cells that were treated with NH_4Cl during the chase. This compound is known to increase pH in intracellular vesicles, thus inhibiting lysosomal degradation (27). As seen in Fig. 5*A*, more receptors were detectable at the end of the 4- and 6-h chase when cells were incubated in the presence of NH_4Cl (compare *lanes 5* and *6* in the *upper* and *lower panels*). The non-*N*-glycosylated receptors were also significantly stabilized with two other lysosomal degradation inhibitors, chloroquine or leupeptin. Importantly, none of these inhibitors had any effect on the wild-type receptor (Fig. 5*B*).

Subcellular localization of the wild-type and non-*N*-glycosylated hδORs was then investigated by confocal microscopy. Cells were induced for 7 h, permeabilized, and labeled with anti-FLAG M2 and anti-calreticulin antibodies. The latter was used as an ER marker. In agreement with our previous results (23), the wild-type hδOR was found to reside mainly in the ER, whereas the non-*N*-glycosylated receptor was almost exclusively localized to the cell surface (Fig. 6, *A–F*). These results are in agreement with the pulse-chase labeling data that showed faster ER export for the non-*N*-glycosylated receptor (see Fig. 2). Trafficking of the cell surface mutant receptors to lysosomes was then studied by adding anti-c-Myc antibody and LysoTrackerRed into the culture medium 4 h before the cells were fixed, permeabilized, and incubated with Alexa-conjugated secondary antibody. Lysosomal degradation was inhibited by adding leupeptin into the medium. In addition to the cell surface, the receptors were now localized strongly in vesicular like structures (Fig. 6, *M–O*), co-localizing partially with the lysosomal marker (see *inset* in Fig. 6*O*). If anti-c-Myc antibody that recognizes the N-terminal extracellular domain of the receptor was replaced with anti-FLAG M2 antibody, which is targeted against the intracellular C terminus, no specific receptor labeling was detected (Fig. 6, *J–L*), confirming the specificity of the anti-c-Myc antibody staining. However, if anti-FLAG M2 antibody was added after permeabilization (Fig. 6, *G–I*), it was able to label the receptors in intracellular vesicles. As most of these receptors were labeled with both anti-FLAG M2 and anti-c-Myc antibodies, it appears that during the 4-h incubation a

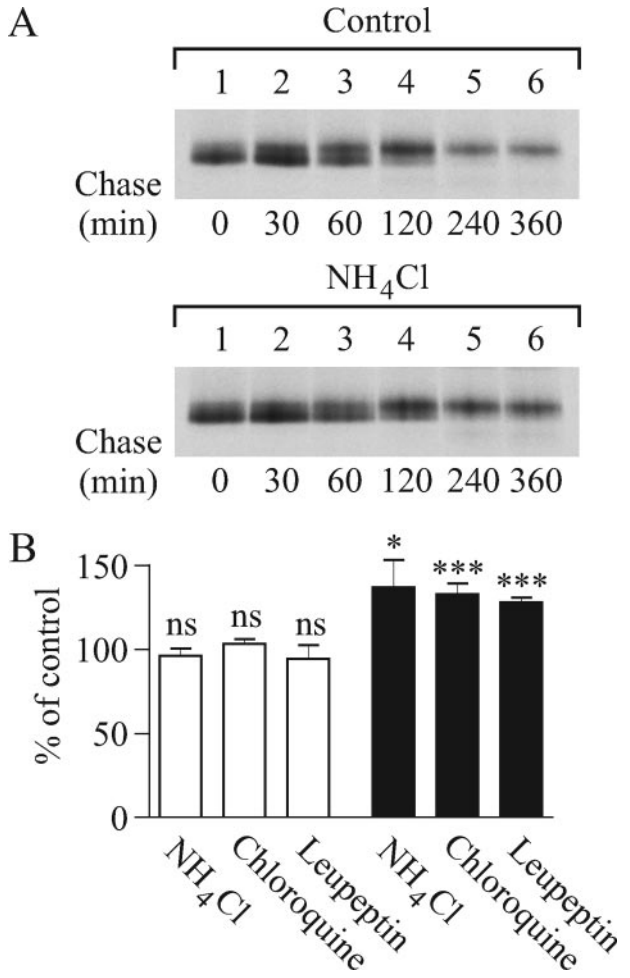

FIGURE 5. **Non-*N*-glycosylated hδORs are degraded in lysosomes.** *A*, HEK293$_t$ cells expressing the hδOR(N18Q/N33Q) were induced to express the receptor for 2 h, pulse-labeled with 100 μCi/ml [^{35}S]methionine/cysteine for 40 min, and chased for increasing periods of time, in the absence or presence of NH_4Cl (10 mM). Alternatively (*B*), HEK293$_t$ cells expressing the wild-type hδOR or the hδOR(N18Q/N33Q) mutant were induced for 17 h, pulse-labeled for 40 min, and chased for 6 h, in the absence or presence of NH_4Cl (10 mM), chloroquine (10 mM), or leupeptin (500 μg/ml). Receptors were purified from total cellular lysates by two-step immunoprecipitation with anti-FLAG M2 antibody, and analyzed by SDS-PAGE and fluorography. Intensities of the labeled mature receptor species were obtained by densitometric scanning of fluorograms, and the values were normalized to the receptor labeling in cells not treated with lysosomal inhibitors. The values given are means ± S.E. of four to six independent experiments. ***, $p < 0.001$; *, $p < 0.05$; *ns*, not significant; *open bars*, wild-type hδOR; *black bars*, hδOR(N18Q/N33Q). The data were analyzed using the unpaired *t* test with GraphPad Prism.

majority of the cell surface receptors was internalized, a finding that was consistent with the results of the constitutive internalization assay (see Fig. 4*A*).

DISCUSSION

All GPCRs, with a couple of exceptions, contain consensus sequences for *N*-glycosylation in their extracellular domains. A large number of these sites are co-translationally occupied by core *N*-glycans that are processed in the ER and Golgi as the receptor molecules are transported to the plasma membrane. An increasing amount of evidence suggests that the *N*-glycans mediate the interaction of nascent receptor molecules with ER glycoprotein quality control components (28–34), preventing misfolded mutant receptors from exiting the ER (28, 31, 32, 35). However, the functional role of *N*-glycans in the scrutiny of newly synthesized wild-type GPCRs has remained obscure. In this study we directly demonstrate the critical role of *N*-glycans for the hδOR, in both receptor folding and quality control.

Several lines of indirect and direct evidence support the important function of the *N*-glycan-mediated quality control of hδORs. (i) Mutation of the two consensus sites for *N*-linked glycosylation at the N-terminal extracellular domain resulted in a receptor that was incapable of interacting with calnexin, disappeared faster from the ER than the wild-type receptor, and was processed to the mature form with enhanced kinetics. Maturation was also facilitated if *N*-glycosylation of the wild-type receptor was prevented by tunicamycin. (ii) Some of the non-*N*-glycosylated receptors that reached the cell surface were incapable of ligand binding. (iii) In addition, the non-*N*-glycosylated receptors showed enhanced turnover and internalization and were targeted for degradation in lysosomes. Consequently, despite the enhanced kinetics of conversion of precursors to the mature form, and facilitated delivery of mature receptors to the cell surface, the steady-state level of hδORs that were devoid of *N*-glycans was lower compared with receptors carrying either one or two *N*-glycans. This was observed whether the receptor expression level was measured by saturation ligand binding, cell surface biotinylation, or flow cytometry.

Reduced expression is a common consequence following the mutation of GPCR *N*-glycosylation sites, and this has often been shown to accompany restricted transport of the mutated receptors to the cell surface and their intracellular accumulation (7–9, 36–39). Nevertheless, for the hδOR this was not the case, and the absence of *N*-glycans actually enhanced the delivery of receptors to the cell surface. The same phenomenon has been reported for temperature-sensitive yeast α-factor receptor mutants, as their trafficking defect was found to be rescued following the mutation of its two *N*-glycosylated asparagine residues (40). Likewise, a recent study on non-*N*-glycosylated κORs (41) has suggested that enhanced ER export may also characterize this receptor, although the mutant receptors were also found to accumulate intracellularly. The reason for the contradictory observations may be related to differences in the folding kinetics of the corresponding proteins, and/or the magnitude of their dependence on *N*-glycan interacting ER chaperones and foldases for the correct folding and processing. The hδOR maturation is a very slow process, and it is therefore understandable that the retention of receptors in the ER is critical for the efficient expression of correctly folded receptors at the cell surface.

The apparent delay in ER export of glycosylated hδORs is most probably caused by lectin-mediated chaperone interactions. The ability of hδORs to interact with calnexin was confirmed by sequential co-immunoprecipitation, and all three *N*-glycosylated receptor forms, but not the non-*N*-glycosylated one, were found to co-purify with calnexin. Previously, calnexin has been shown to be involved in ER retention of mutant GPCRs, like the human V2 vasopressin receptor (28), and more recently it has also been found to interact with a number of wild-type GPCRs (*e.g.* see Refs. 30–34). In this study, the efficiency of co-purification with calnexin was decreased for hδOR

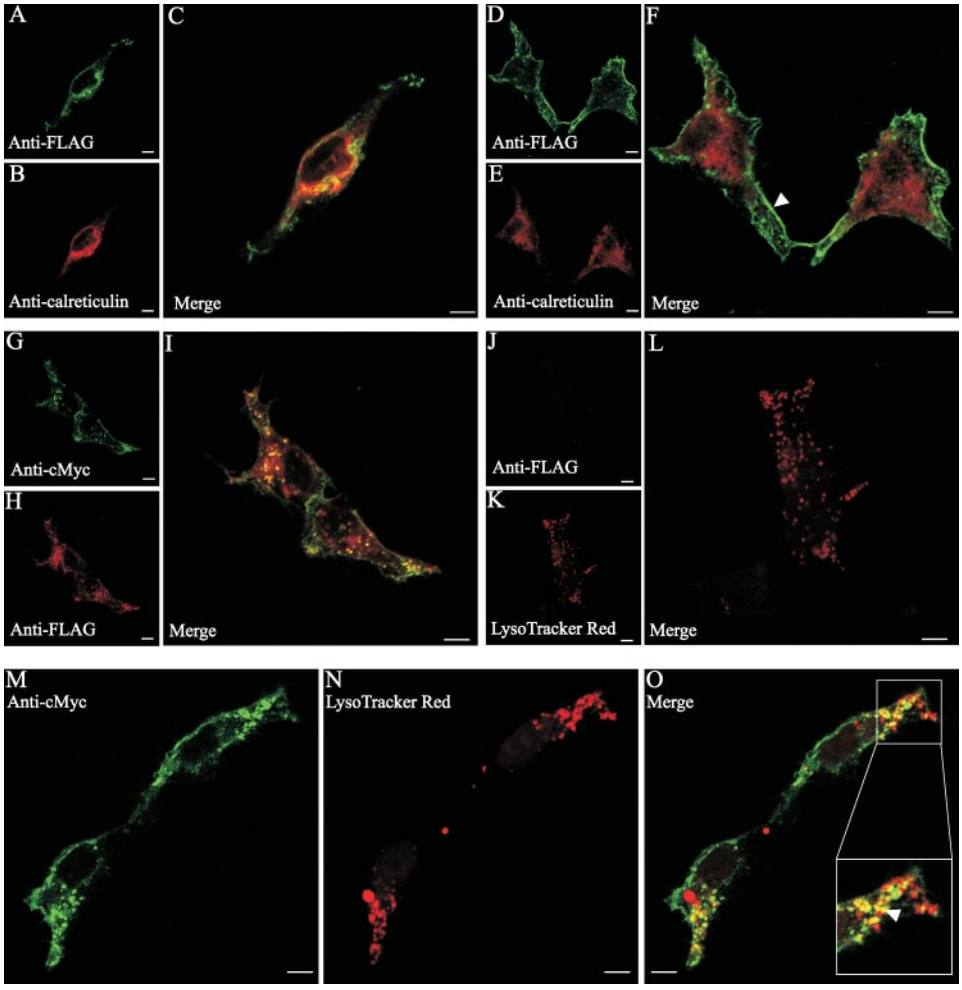

FIGURE 6. **Internalized non-*N*-glycosylated hδORs are transported into lysosomal vesicles.** HEK293$_t$ cells expressing the wild-type hδOR (*A–C*) or the N18Q/N33Q mutant (*D–O*) were induced for 7 h, in the absence (*A–F*) or presence (*G–O*) of leupeptin (500 μg/ml), which was added into the culture medium 60 min after tetracycline. Anti-c-Myc (A-14) (*G–I* and *M–O*) or anti-FLAG M2 (*J–L*) antibodies were added into the medium 4 h before cells were fixed, and the lysosomal marker LysoTrackerRed was added simultaneously to a final concentration of 200 nM (*J–O*). After fixation and permeabilization, the internalized antibodies were labeled with the corresponding secondary antibodies: Alexa488-conjugated goat anti-rabbit (*G–I* and *M–O*) or anti-mouse (*J–L*) antibodies. Alternatively, cells were stained with anti-FLAG M2 (*A–I*) or anti-calreticulin (*A–F*) antibodies after permeabilization, followed by Alexa 488- or Alexa 568-conjugated goat anti-mouse (*A–F* and *G–I*, respectively) and Alexa 568-conjugated goat anti-rabbit (*A–F*) IgGs. The *arrowheads* in *F* and *O* indicate receptors at the cell surface and in intracellular vesicles that contain the lysosomal marker, respectively. *Bars,* 5 μm.

species that contained only one *N*-glycan, and this was particularly evident for the wild-type receptor. This may reflect a genuine difference in the binding affinity of calnexin for the different receptor forms, as it has been demonstrated earlier that the efficient binding of calnexin to glycoproteins takes place only if at least two core *N*-glycans are attached to the nascent protein (42, 43).

It has been reported previously that *N*-glycans that are attached to newly synthesized glycoproteins are not necessarily equally important for folding and ER retention (12, 36, 37, 44–46). This appears to apply also to the hδOR, as the N18Q mutant, unlike the N33Q one, resembled the double mutant in that its maturation kinetics was enhanced compared with the wild-type receptor. This implies that the second *N*-glycosylation site at Asn^{33} is more critical for ER retention of the hδOR. This *N*-glycosylation site seems to be conserved in the opioid receptor family (J. Tuusa, Blast, ClustalW multiple sequence alignments). Surprisingly, despite the obvious importance of this *N*-glycosylation site, it was used inefficiently, and some of the wild-type hδORs harbored carbohydrate only at Asn^{18}. Similarly, the N18Q mutant existed partially in a nonglycosylated form at the cell surface. The reason for this phenomenon is not known at present but may be related to local differences in the amino acid sequence close to the consensus site (47–49) or to its closer proximity to the membrane (50). For example, studies with the tissue-type plasminogen activator and hemagglutinin-neuraminidase glycoprotein of the Newcastle disease virus indicate that events affecting the local folding of a polypeptide chain (*e.g.* disulfide bond formation) may limit the accessibility of consensus site asparagines to oligosaccharyltransferase (51, 52). Differences in the local environment of the glycosylated asparagines of the hδOR may also explain the divergent Golgi processing of the two *N*-glycans, which was suggested by the observation that mature forms of the N33Q and N18Q mutants displayed a clear difference in electrophoretic mobility, a difference that was not explained by *O*-glycosylation. Interestingly, a similar difference in mobility was also seen for the κOR, when either one of its two glycosylated asparagines was mutated to glutamine (41).

A fraction of the non-*N*-glycosylated hδORs that reached the cell surface appeared to exist in a conformation that was not compatible with ligand binding. This was demonstrated by the fact that fluorescein-NTX was able to recognize a smaller population of cell surface receptors than c-Myc antibody, whereas no such difference was observed for receptors carrying at least one *N*-glycan. In previous studies, only a very few other glycoproteins have been shown to be able to exit the ER in an incorrect conformation. One of these is human tripeptidyl-peptidase I, a lysosomal enzyme that was found to be secreted with non-native disulfide bonds and only with limited activity after mutation of one of its five *N*-glycosylation sites (46).

The mature non-*N*-glycosylated hδORs were also found to have a faster turnover than the wild-type receptors. Furthermore, they were considerably more prone to internalization and were targeted for lysosomal degradation, as was demonstrated by flow cytometry, metabolic pulse-chase labeling, and confocal microscopy. Importantly, the agonist-mediated inter-

nalization of the non-*N*-glycosylated receptors was also enhanced compared with wild-type receptors, suggesting that not only misfolded but also folding-competent mutant receptors were prone to efficient disposal from the cell surface. This is most likely explained by the absence of *N*-glycan-mediated stabilization of cell surface receptors, as has been reported for numerous other proteins (53), including the non-*N*-glycosylated κOR that also internalizes more efficiently after agonist-mediated activation (41). However, no significant differences in the structural stability were observed for the wild-type and non-*N*-glycosylated hδORs in the heat inactivation assay, possibly reflecting the inability of the *in vitro* assay to recapitulate *in vivo* conditions and events that take place in living cells. In any case, it is tempting to speculate that a distinct functional quality control machinery exists at the cell surface that is able to target unstable and/or misfolded receptors for disposal, a mechanism that has also been proposed to dispose other polytopic membrane proteins, like misfolded cystic fibrosis transmembrane conductance regulator and yeast plasma membrane ATPase Pma1 (54, 55). The structural determinants that target the non-*N*-glycosylated hδORs for degradation remain to be determined in future studies. It is very likely that the quality control machinery relies on conformational attributes rather than merely on the absence of *N*-glycans.

In conclusion, this study expands our knowledge on GPCR biosynthesis and highlights the importance of *N*-glycan-mediated ER quality control in ensuring that newly synthesized GPCRs fold correctly before they are inserted into the plasma membrane. In addition, it accentuates the additional structural stability that the *N*-glycans provide at the cell surface. It can be envisioned that ER glycoprotein quality control is especially vital for receptors that require extended periods of time to find their correct conformation in the ER, emphasizing the need for more thorough investigation on the functional significance of *N*-glycosylation for GPCR biosynthesis and trafficking.

Acknowledgments—We thank Paula Salmela, Miia Vierimaa, Seija Leskelä, and Liisa Kärki for skillful technical assistance. We are also grateful to other members of the GPCR team for fruitful discussions and critical reading of the manuscript.

REFERENCES

1. Ellgaard, L., and Helenius, A. (2003) *Nat. Rev. Mol. Cell Biol.* **4,** 181–191
2. Trombetta, E. S., and Parodi, A. J. (2003) *Annu. Rev. Cell Dev. Biol.* **19,** 649–676
3. Helenius, A., and Aebi, M. (2004) *Annu. Rev. Biochem.* **73,** 1019–1049
4. Ruddock, L. W., and Molinari, M. (2006) *J. Cell Sci.* **119,** 4373–4380
5. Landolt-Marticorena, C., and Reithmeier, R. A. (1994) *Biochem. J.* **302,** 253–260
6. Couvineau, A., Fabre, C., Gaudin, P., Maoret, J. J., and Laburthe, M. (1996) *Biochemistry* **35,** 1745–1752
7. Deslauriers, B., Ponce, C., Lombard, C., Larguier, R., Bonnafous, J. C., and Marie, J. (1999) *Biochem. J.* **339,** 397–405
8. Böer, U., Neuschäfer-Rube, F., Möller, U., and Püschel, G. P. (2000) *Biochem. J.* **350,** 839–847
9. Lanctôt, P. M., Leclerc, P. C., Escher, E., Leduc, R., and Guillemette, G. (1999) *Biochemistry* **38,** 8621–8627
10. van Koppen, C. J., and Nathanson, N. M. (1990) *J. Biol. Chem.* **265,** 20887–20892
11. Fukushima, Y., Oka, Y., Saitoh, T., Katagiri, H., Asano, T., Matsuhashi, N., Takata, K., van Breda, E., Yazaki, Y., and Sugano, K. (1995) *Biochem. J.* **310,** 553–558
12. Kaushal, S., Ridge, K. D., and Khorana, H. G. (1994) *Proc. Natl. Acad. Sci. U. S. A.* **91,** 4024–4028
13. Waldhoer, M., Bartlett, S. E., and Whistler, J. L. (2004) *Annu. Rev. Biochem.* **73,** 953–990
14. Petäjä-Repo, U. E., Hogue, M., Laperrière, A., Walker, P., and Bouvier, M. (2000) *J. Biol. Chem.* **275,** 13727–13736
15. Petäjä-Repo, U. E., Hogue, M., Leskelä, T. T., Markkanen, P. M. H., Tuusa, J. T., and Bouvier, M. (2006) *J. Biol. Chem.* **281,** 15780–15789
16. Petäjä-Repo, U. E., Hogue, M., Laperrière, A., Bhalla, S., Walker, P., and Bouvier, M. (2001) *J. Biol. Chem.* **276,** 4416–4423
17. Petäjä-Repo, U. E., Hogue, M., Bhalla, S., Laperrière, A., Morello, J. P., and Bouvier, M. (2002) *EMBO J.* **21,** 1628–1637
18. Leskelä, T. T., Markkanen, P. M. H., Pietilä, E. M., Tuusa, J. T., and Petäjä-Repo, U. E. (2007) *J. Biol. Chem.* **282,** 23171–23183
19. Apaja, P. M., Tuusa, J. T., Pietilä, E. M., Rajaniemi, H. J., and Petäjä-Repo, U. E. (2006) *Mol. Biol. Cell* **17,** 2243–2255
20. Frang, H., Mukkala, V. M., Syystö, R., Ollikka, P., Hurskainen, P., Scheinin, M., and Hemmilä, I. (2003) *Assay Drug Dev. Technol.* **1,** 275–280
21. Pietilä, E. M., Tuusa, J. T., Apaja, P. M., Aatsinki, J. T., Hakalahti, A. E., Rajaniemi, H. J., and Petäjä-Repo, U. E. (2005) *J. Biol. Chem.* **280,** 26622–26629
22. Guan, X. M., Kobilka, T. S., and Kobilka, B. K. (1992) *J. Biol. Chem.* **267,** 21995–21998
23. Tuusa, J. T., Markkanen, P. M. H., Apaja, P. M., Hakalahti, A. E., and Petäjä-Repo, U. E. (2007) *J. Mol. Biol.* **371,** 622–638
24. Knapp, R. J., Malatynska, E., Collins, N., Fang, L., Wang, J. Y., Hruby, V. J., Roeske, W. R., and Yamamura, H. I. (1995) *FASEB J.* **9,** 516–525
25. McDowell, W., and Schwarz, R. T. (1988) *Biochimie* (*Paris*) **70,** 1535–1549
26. Gether, U., Ballesteros, J. A., Seifert, R., Sanders-Bush, E., Weinstein, H., and Kobilka, B. K. (1997) *J. Biol. Chem.* **272,** 2587–2590
27. Seglen, P. O., Grinde, B., and Solheim, A. E. (1979) *Eur. J. Biochem.* **95,** 215–225
28. Morello, J. P., Salahpour, A., Petäjä-Repo, U. E., Laperrière, A., Lonergan, M., Arthus, M. F., Nabi, I. R., Bichet, D. G., and Bouvier, M. (2001) *Biochemistry* **40,** 6766–6775
29. Siffroi-Fernandez, S., Giraud, A., Lanet, J., and Franc, J. L. (2002) *Eur. J. Biochem.* **269,** 4930–4937
30. Lu, M., Echeverri, F., and Moyer, B. D. (2003) *Traffic* **4,** 416–433
31. Mizrachi, D., and Segaloff, D. L. (2004) *Mol. Endocrinol.* **18,** 1768–1777
32. Robert, J., Auzan, C., Ventura, M. A., and Clauser, E. (2005) *J. Biol. Chem.* **280,** 42198–42206
33. Rosenbaum, E. E., Hardie, R. C., and Colley, N. J. (2006) *Neuron* **49,** 229–241
34. Free, R. B., Hazelwood, L. A., Cabrera, D. M., Spalding, H. N., Namkung, Y., Rankin, M. L., and Sibley, D. R. (2007) *J. Biol. Chem.* **282,** 21285–21300
35. Fan, J., Perry, S. J., Gao, Y., Schwarz, D. A., and Maki, R. A. (2005) *Mol. Endocrinol.* **19,** 2579–2590
36. Ray, K., Clapp, P., Goldsmith, P. K., and Spiegel, A. M. (1998) *J. Biol. Chem.* **273,** 34558–34567
37. Karpa, K. D., Lidow, M. S., Pickering, M. T., Levenson, R., and Bergson, C. (1999) *Mol. Pharmacol.* **56,** 1071–1078
38. Webel, R., Menon, I., O'Tousa, J. E., and Colley, N. J. (2000) *J. Biol. Chem.* **275,** 24752–24759
39. Michineau, S., Muller, L., Pizard, A., Alhenc-Gélas, F., and Rajerison, R. M. (2004) *Biol. Chem.* **385,** 49–57
40. Mentesana, P. E., and Konopka, J. B. (2001) *Biochemistry* **40,** 9685–9694
41. Li, J. G., Chen, C., and Liu-Chen, L. Y. (2007) *Biochemistry* **46,** 10960–10970
42. Branza-Nichita, N., Negroiu, G., Petrescu, A. J., Garman, E. F., Platt, F. M., Wormald, M. R., Dwek, R. A., and Petrescu, S. M. (2000) *J. Biol. Chem.* **275,** 8169–8175
43. Deprez, P., Gautschi, M., and Helenius, A. (2005) *Mol. Cell* **19,** 183–195
44. Hebert, D. N., Zhang, J. X., Chen, W., Foellmer, B., and Helenius, A. (1997) *J. Cell Biol.* **139,** 613–623
45. Benya, R. V., Kusui, T., Katsuno, T., Tsuda, T., Mantey, S. A., Battey, J. F., and Jensen, R. T. (2000) *Mol. Pharmacol.* **58,** 1490–1501
46. Wujek, P., Kida, E., Walus, M., Wisniewski, K. E., and Golabek, A. A.

(2004) *J. Biol. Chem.* **279,** 12827–12839
47. Mellquist, J. L., Kasturi, L., Spitalnik, S. L., and Shakin-Eshleman, S. H. (1998) *Biochemistry* **37,** 6833–6837
48. Elliott, S., Chang, D., Delorme, E., Eris, T., and Lorenzini, T. (2004) *J. Biol. Chem.* **279,** 16854–16862
49. Petrescu, A. J., Milac, A. L., Petrescu, S. M., Dwek, R. A., and Wormald, M. R. (2004) *Glycobiology* **14,** 103–114
50. Nilsson, I. M., and von Heijne, G. (1993) *J. Biol. Chem.* **268,** 5798–5801
51. Allen, S., Naim, H. Y., and Bulleid, N. J. (1995) *J. Biol. Chem.* **270,** 4797–4804
52. McGinnes, L. W., and Morrison, T. G. (1997) *J. Virol.* **71,** 3083–3089
53. Imperiali, B., and O'Connor, S. E. (1999) *Curr. Opin. Chem. Biol.* **3,** 643–649
54. Sharma, M., Pampinella, F., Nemes, C., Benharouga, M., So, J., Du, K., Bache, K. G., Papsin, B., Zerangue, N., Stenmark, H., and Lukacs, G. L. (2004) *J. Cell Biol.* **164,** 923–933
55. Liu, Y., Sitaraman, S., and Chang, A. (2006) *J. Biol. Chem.* **281,** 31457–31466